

Disk-based enzyme-linked immunosorbent assays using the liquid-aliquoting and siphoning-evacuation technique

Ho-Chin Wu, Yen-Hao Chen, and Chih-Hsin Shih

Department of Chemical Engineering, Feng Chia University, 40724 Taichung, Taiwan

(Received 6 July 2018; accepted 28 August 2018; published online 13 September 2018)

A cost-effective way to carry out multiple enzyme-linked immunosorbent assays (ELISAs) on a centrifugal platform using the liquid-aliquoting and siphoning-evacuation (LASE) technique was developed in this paper. Instead of preloading all the reagents in the reservoirs before testing, each reagent was loaded only one time during testing. The reagent was distributed into equal aliquots and delivered into reaction chambers by the aliquoting fluidic function. In addition, a siphoning-evacuation technique was developed to improve the washing efficiency and simplify the assay protocol. Furthermore, the entire assay protocol can be conducted using a two-step spinning protocol, which greatly reduces the cost of the motor control system. With the LASE technique, a low-cost and user-friendly ELISA system can be achieved. Published by AIP Publishing. <https://doi.org/10.1063/1.5047281>

INTRODUCTION

The enzyme-linked immunosorbent assay (ELISA), a technique used to detect the presence of antibodies or antigens in a sample, is widely used in biomedical and biochemical diagnoses. In the current practice, the ELISA is mostly conducted using the microtiter plate and its operating procedure is both labor-intensive and time-consuming.^{1–7} In order to facilitate the assay operation, many disk-based ELISA platforms were developed in the past few years.^{1–5,8–16} In most of the disk-based ELISA platforms, reagents were required to be loaded onto the disk before testing, and then the sequential addition of the reagents was carried out by integrating the spinning protocol with various valving techniques such as capillary burst valves,^{2–4,6,7} wax valves,^{9,11,17} pneumatic valves,^{8,18–22} and siphoning valves.^{18,23} It has been demonstrated that a complete ELISA procedure can be conducted in automation on a disk-based platform.^{2–4,8,11,14} However, in these systems, a programmable and precise spinning control is usually required, which makes the systems expensive and difficult to commercialize. In addition, in order to increase the throughput and reduce the cost of the assay, it is recommended that one place multiple assay fluidics on the disk platform. Accordingly, the number of reagent loading steps is also drastically increased, which makes the operating procedure of the disk-based ELISA tedious and unfriendly to use.

Moreover, the ELISA protocol usually involves multiple washing steps in order to remove non-specific binding of antigens or antibodies and improve the signal-to-noise ratio of the assay. Conventionally, washing steps on the centrifugal platform were mostly conducted by the liquid-replacement approach. A large volume of wash buffer was used to replace the liquid residing in the reaction chamber.^{1–4,6,7} Consequently, large-sized wash buffer reservoirs and waste chambers were also required, which reduced the number of assay fluidics on a disk platform. In addition to the liquid-replacement approach, the liquid-evacuation approach, which is performed by evacuating the liquid in the reaction chamber before adding another liquid, has been demonstrated by using wax valves^{9,11,14} and push-pull pumping by thermally induced expansion and contraction of the air in a closed chamber.⁸ Compared to the liquid-replacement approach, the liquid-evacuation approach might improve the washing efficiency by reducing the amount of residue from the liquid previously residing in the reaction chamber. However, in the above-mentioned literature, an external energy source was required to melt the wax or heat up the air in the liquid evacuation process. It would increase the complexity and cost of the assay in operation.

In order to provide an inexpensive and more user-friendly platform, a novel approach to conduct the disk-based ELISA using the liquid-aliquoting and siphoning-evacuation (LASE) technique was developed in this study. In this platform, the sample loading procedure is facilitated by an aliquoting fluidic design. Each reagent only needs to be loaded once and the aliquoting fluidic structure delivers the reagent into multiple reaction chambers. In addition, a liquid-evacuation approach by siphoning was developed to improve the washing efficiency. The mechanisms for liquid aliquoting and flow control in both incubation and evacuation processes are also discussed. Our goal is to provide a low-cost and user-friendly platform for the point-of-care market.

EXPERIMENTAL

Materials

Monoclonal mouse anti-human chorionic gonadotropin (hCG) antibody and horseradish peroxidase (HRP) conjugated monoclonal mouse anti-hCG antibody were purchased from BioCheck (Foster City, CA, USA) and used as the capture and detection antibodies. The 3,3',5,5'-tetramethylbenzidine (TMB) substrate was purchased from SurModics (Eden Prairie, MN, USA). Phosphate buffered saline (PBS), Tween-20, 1-ethyl-3-[3-dimethylaminopropyl] carbodiimide hydrochloride (EDC), 2-(N-morpholino) ethane sulfonic acid (MES), bovine serum albumin (BSA), and ProClin 300 were purchased from Sigma-Aldrich. *N*-hydroxysuccinimide (NHS) was obtained from Alfa Aesar (Haverhill, MA, USA). The super-paramagnetic beads (TANBeads U-128) were purchased from Taiwan Advanced Nanotech (Taiwan). The wash buffer was made by adding 1% Tween-20 in PBS. The storage buffer was made by adding 0.5% BSA, 0.05% Tween-20, and 0.02% ProClin 300 in PBS.

Functional magnetic beads preparation

To prepare the antibody conjugated magnetic beads, the super-paramagnetic beads ($75\ \mu\text{l}$, $50\ \text{mg}/\text{ml}$) were incubated in a mixture of MES buffer ($500\ \mu\text{l}$, $25\ \text{mM}$, pH 5.0) and ddH₂O ($500\ \mu\text{l}$) for 10 min. After removing the supernatant, the magnetic beads were incubated with EDC ($250\ \mu\text{l}$, $100\ \text{mg}/\text{ml}$) and NHS ($250\ \mu\text{l}$, $100\ \text{mg}/\text{ml}$) for 30 min with vortexing at room temperature. The magnetic beads were washed twice with MES buffer ($500\ \mu\text{l}$) and then incubated with the mixture of monoclonal mouse anti-hCG antibody ($50\ \mu\text{l}$, $1\ \text{mg}/\text{ml}$) and MES buffer ($450\ \mu\text{l}$, $25\ \text{mM}$) for 60 min with vortexing at room temperature. Later, the magnetic beads were incubated with the Tris buffer ($500\ \mu\text{l}$, $50\ \text{mM}$, pH 7.4) for 15 min. Finally, the Tris buffer was removed and the magnetic beads were washed 4 times with PBS ($500\ \mu\text{l}$) and then stored in the storage buffer (pH 7.4) at $4\ ^\circ\text{C}$.

Disk fabrication and flow visualization

The microfluidic disk is composed of two layers. The bottom layer is a polymethylmethacrylate disk (80 mm in diameter and 3 mm thick) with microstructures engraved by an automatic engraving machine (EGX-350, Roland, USA). The top layer is a clear polyolefin film coated with a pressure-sensitive silicone-based adhesive (9795R, 3M, USA). The surface of the disk was treated with oxygen plasma before packaging to render the siphoning channel hydrophilic. The motor control system, which is capable of conducting precise spinning control and is used to evaluate the performance of the fluidic function, was mentioned in our previous work.^{7,24} To observe the fluid flow under rotation, a high-speed complementary metal oxide semiconductor camera (AVT BONITO CL-400C, Allied Vision, USA) and a stroboscope (DT-311N, SHIMPO, Japan) were used to capture images of the disk at the same location. The images were analyzed using computer software (Vision Assistant 2015, Nation Instrument, USA) to acquire information required for liquid volume quantification and flow field analysis.

Low-cost centrifugal analyzer

The low-cost centrifugal analyzer was made by modifying a mini centrifuge (Select BioProducts, USA). As shown in Fig. 1, a speed governor (ADIO-E3A1, Tun-Hwa Electronic

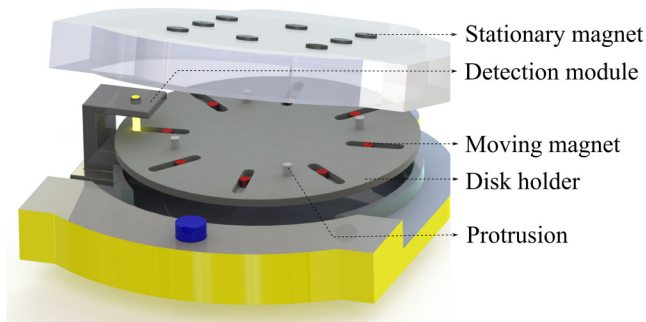


FIG. 1. The schematic of a low-cost centrifugal analyzer. It was made by adding a stationary magnet stage, a disk holder, and a detection unit on a mini centrifuge.

Material, Taiwan) was added to the motor so that the rotational speed of the motor can be tunable from 10 to 4000 RPM. Since only two rotational speeds were required in the assay protocol, a switch was installed so that the mini centrifuge could be operated at either high (2500 RPM) or low (10 RPM) rotational speeds. The detection unit, which consisted of a LED (600 nm) and a photodiode (BPW34, SIEMENS, Taiwan), was installed on the mini centrifuge for signal detection.

To facilitate the movement of magnetic beads, a stationary magnet stage, which was composed of several permanent magnets, was installed on the cover of the mini centrifuge. In addition, the rotor of the mini centrifuge was replaced by a disk holder which contained eight moving rails with one moving magnet inside each moving rail. The movement of the moving magnet was governed by the rotational speed of the disk holder and its position relative to the stationary magnets.⁷ Furthermore, four cylindrical protrusions, which matched the position of the holes on the disk, were installed on the disk holder. During spinning, the disk could be fixed steadily through the engagement between the holes and the cylindrical protrusions.

MICROFLUIDIC FUNCTIONS

Aliquoting

The reagent loading process is usually tedious and time-consuming when multiple tests are conducted simultaneously on one disk platform. To reduce the number of reagent loading steps, an aliquoting design, which is capable of evenly distributing the reagent to individual reaction chambers, was developed. As shown in Fig. 2(a), the aliquoting structure includes a central reservoir at the center of the disk and eight aliquoting chambers which are connected to eight reaction chambers through straight channels. Burst valves, which are used to stop the flow at low rotational speed, are located between the junction of the aliquoting chamber and the straight channel.

The aliquoting structure is placed at the center of the disk to prevent uneven liquid distribution resulted from the Coriolis force.^{25,26} In addition, the aliquoting structure can be used to aliquot liquids of different volumes, such as the wash buffer and substrate solution, which are regularly used in an immunoassay. Furthermore, since most of the reagents are aliquoted by the same structure, the space saved from the reagent reservoirs can be used to accommodate more assay fluidics on the disk platform.

To evaluate the effectiveness of the aliquoting structure, a series of experiments were conducted by varying the angular acceleration of the disk, reservoir height, and volume-filling ratio, which is defined by the ratio of liquid volume to the space of the central reservoir. The aliquoting efficiency is represented by the coefficient of variation (CV) of the aliquoted volumes in eight reaction chambers. Low CV represents good aliquoting efficiency. Figure 2(b) shows the effects of the angular acceleration of the disk and the reservoir height on the variation of the aliquoted volumes in eight chambers at the filling ratio of 70%. The CV of the aliquoted volumes decreases as the angular acceleration and chamber height increase. Higher Euler force and lower flow resistance

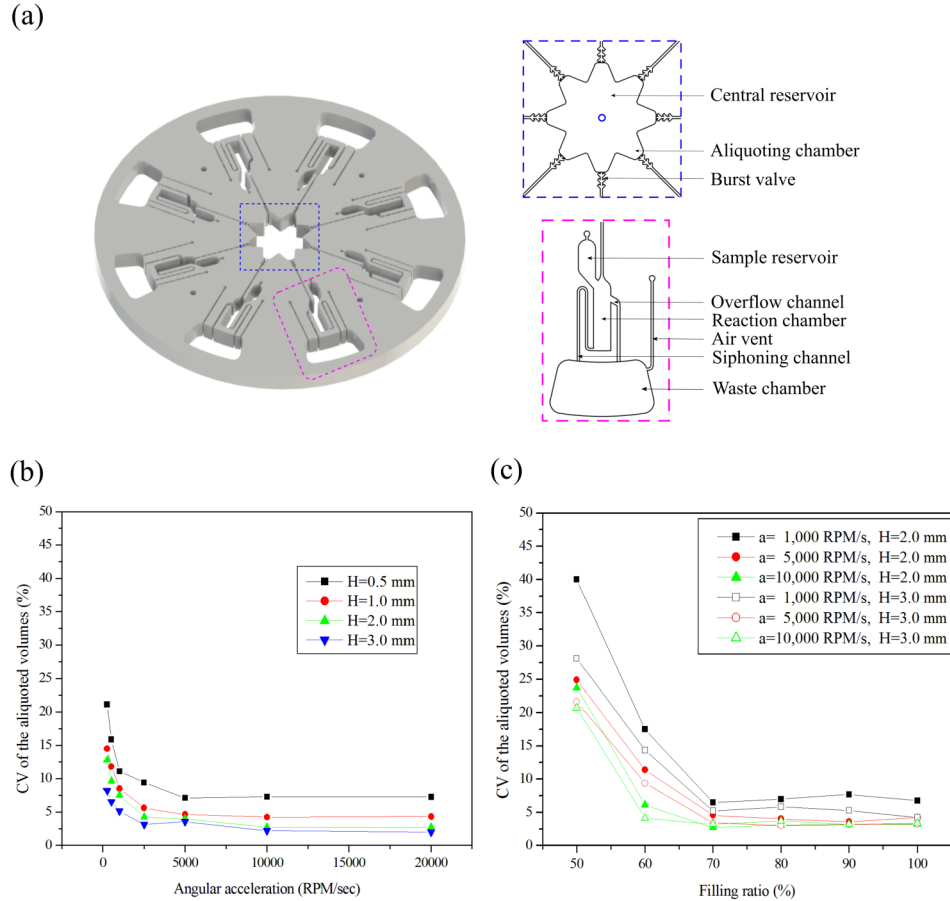


FIG. 2. (a) The schematic illustration of the aliquoting fluidic design for ELISA. (b) The effect of the angular acceleration of the disk on the variation of the aliquoted volumes under various reservoir heights at the filling ratio of 70%. (c) The effect of filling ratio on the variation of the aliquoted volumes under various angular accelerations and reservoir heights.

seem to benefit the liquid distribution and result in lower variation in the aliquoted volumes. In addition, the CV of the aliquoted volumes does not change significantly when the angular acceleration is above 5000 RPM/s and when the chamber height is above 2 mm. Figure 2(c) shows the effect of filling ratio on the variation of the aliquoted volumes under various reservoir heights and angular accelerations. The CV of the aliquoted volumes decreases as the filling ratio increases. However, the CV does not decrease significantly when the filling ratio is above 70%.

In conclusion, low CV of the aliquoted volumes can be achieved at high angular velocities, large reservoir heights, and high filling ratios. To explore the limitation of the aliquoting function, the above experiments were conducted using a motor control system whose angular acceleration can be elevated up to 50 000 RPM/s. However, the motor used for the low-cost analyzer could only reach the angular acceleration of 1000 RPM/s; therefore, the filling ratio of 70% and chamber height of 2 mm were chosen in the following experiments in order to achieve relatively low CV with a reasonable filling ratio.

Siphoning evacuation

An ELISA protocol usually involves several liquid adding, incubating, and removing steps for the reagents and wash buffer in order to improve the sensitivity of the assay. As mentioned earlier, the conventional liquid-replacement approach usually requires a large volume of wash buffer and/or many washing steps in order to achieve decent washing efficiency. In this work, we proposed a siphoning-evacuation design which is capable of evacuating the liquid in the reaction chamber

before another liquid is added and governing the residence time of the reagent in the reaction chamber.

The mechanism of the siphoning-evacuation approach is shown in Fig. 3. The liquid was loaded into the central reservoir and delivered to the reaction chamber under a high rotational speed (ω_H) [Fig. 3(a)]. During incubation, the rotational speed of the disk was reduced to a low rotational speed (ω_L). Since the centrifugal force was no longer prevailing over the capillary force in the siphoning channel, the liquid primed the siphoning channel and eventually stopped at the exit of the siphoning channel due to the capillary valving effect [Fig. 3(b)]. At this moment, since the air/liquid interface at the exit of the siphoning channel was lower than the air/liquid interface in the reaction chamber, increasing the rotational speed of the disk to ω_H would drain the liquid from the reaction chamber into the waste chamber and evacuate the reaction chamber.

The magnitude of ω_H in the evacuation process played an important role in the liquid flow control. If ω_H was lower than the critical rotational speed (ω_C), the liquid remained in the siphoning channel after the evacuating process [Fig. 3(c)]. When the next liquid was delivered into the reaction chamber at ω_H , it would be drained into the waste chamber immediately by the siphoning effect and resulted in an empty reaction chamber [Fig. 3(d)]. Accordingly, the residence time for the newly added liquid would be very short, which is not suitable for the incubation process. On the other hand, if ω_H was higher than ω_C , air would flow into the inlet of the siphoning channel from the reaction chamber and the liquid in the siphoning channel would be drained into the waste chamber during the evacuating process [Fig. 3(e)]. When the next liquid was delivered into the reaction chamber at ω_H , it would stay in the reaction chamber for the incubation process [Fig. 3(f)]. The incubation and washing steps can be carried out more efficiently when a proper high rotational speed was chosen.

The critical rotational speed (ω_C), which governed the residence time of the newly added liquid, is described in Fig. 4(a). At the end of the siphoning-evacuation process, most of the liquid

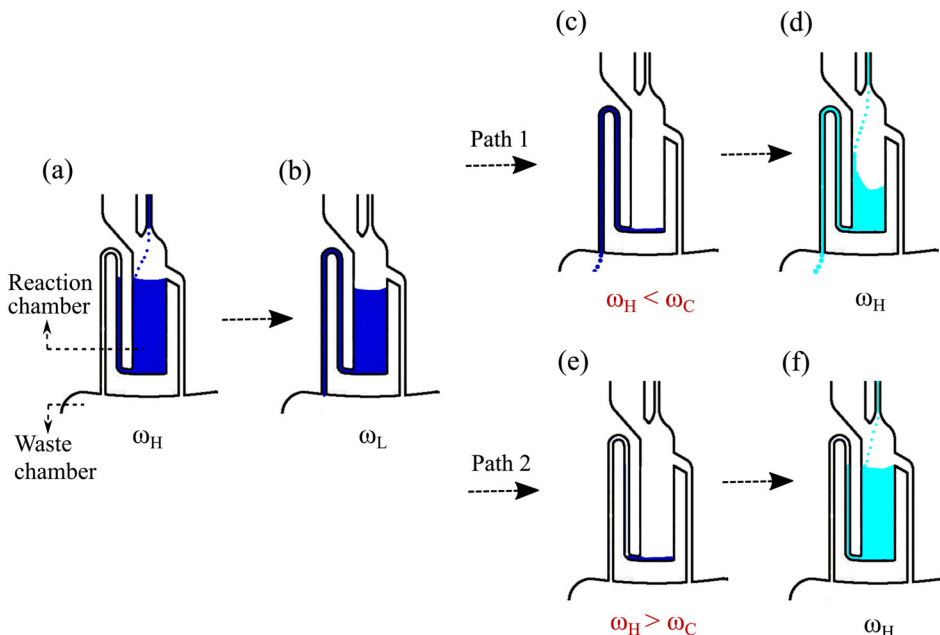


FIG. 3. The mechanism of the siphoning-evacuation approach. (a) The reaction chamber was filled with liquid at ω_H . (b) By reducing the rotational speed to ω_L , the liquid primed the siphoning channel by the capillary action and stopped at the exit of the siphoning channel. (c) In path 1, by increasing the rotational speed to ω_H ($\omega_H < \omega_C$), the liquid from the reaction chamber was drained into the waste chamber while the siphoning channel was filled with liquid. (d) The newly added liquid would be drained from the reaction chamber into the waste chamber immediately. (e) In path 2, by increasing the rotational speed to ω_H ($\omega_H > \omega_C$), the liquid was drained from the reaction chamber into the waste chamber and the siphoning channel was filled with air. (f) When the liquid was added to the reaction chamber at ω_H , it stayed in the reaction chamber.

in the reaction chamber was drained into the waste chamber and the air/liquid interface in the reaction chamber approached to the inlet of the siphoning channel. At this moment, the air/liquid interface at the exit of the siphoning channel was balanced by the centrifugally induced pressure ΔP_c and the surface tension induced pressure ΔP_s .⁶

$$\Delta P_c = \rho_c^2 \bar{R} \Delta R, \quad (1)$$

$$\Delta P_s = \frac{4\gamma \sin \theta}{d_H}, \quad (2)$$

where ρ is the density of the liquid, ω_c is the critical rotational speed, γ is the surface tension of the liquid, θ is the contact angle, d_H is the hydraulic diameter of the siphoning channel, \bar{R} is the average of R_1 and R_2 , and ΔR is the difference between R_1 and R_2 . R_1 and R_2 are the inner and the outer radii of the liquid element in the reaction chamber and the capillary channel, respectively.

According to the equations, the critical rotational speed at the exit of the siphoning channel can be expressed as

$$\omega_c = \left(\frac{4\gamma \sin \theta}{\rho \bar{R} \Delta R \rho d_H} \right)^{0.5}. \quad (3)$$

When the rotational speed of the disk was increased to be higher than the critical rotational speed ($\omega > \omega_c$), the air/liquid interface in the reaction chamber would move further outward in the radial direction and resulted in the removal of the liquid in the siphoning channel by letting the air flow into siphoning channel.

To verify this theory, experiments were carried out by varying the hydraulic diameter (d_H : 0.2–0.8 mm) and the radial position of the siphoning channel (R : 10–40 mm) while keeping $\Delta R = 2$ mm. As shown in Fig. 4(b), the critical rotational speed from the experimental data

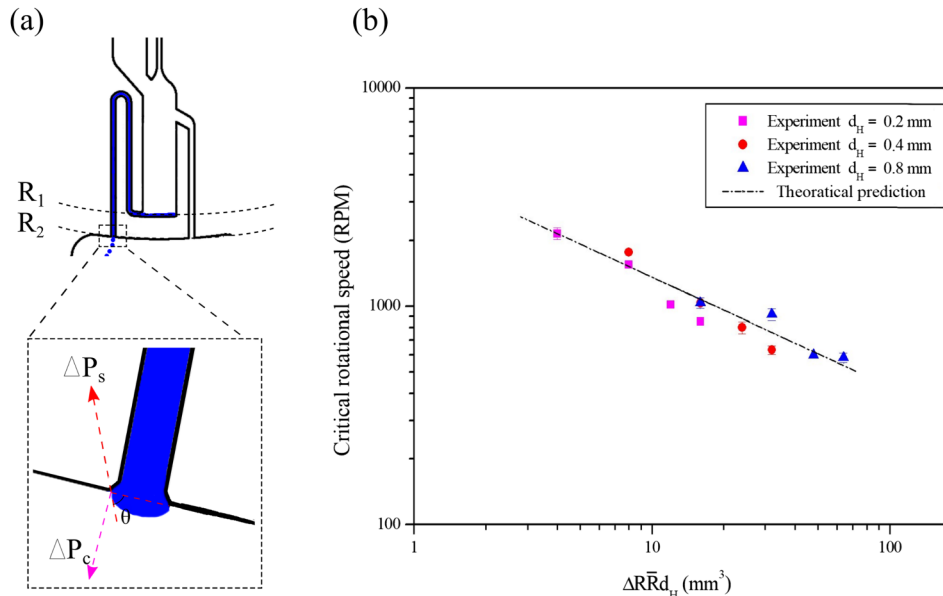


FIG. 4. (a) Schematic illustration of the liquid element in the siphoning channel at the end of the liquid-evacuation process. The air/liquid interface near the exit of the outlet was balanced by the centrifugally induced pressure (ΔP_c) and the surface tension induced pressure (ΔP_s). (b) The measured critical rotational speed from the experimental data for various hydraulic diameters of the siphoning channel.

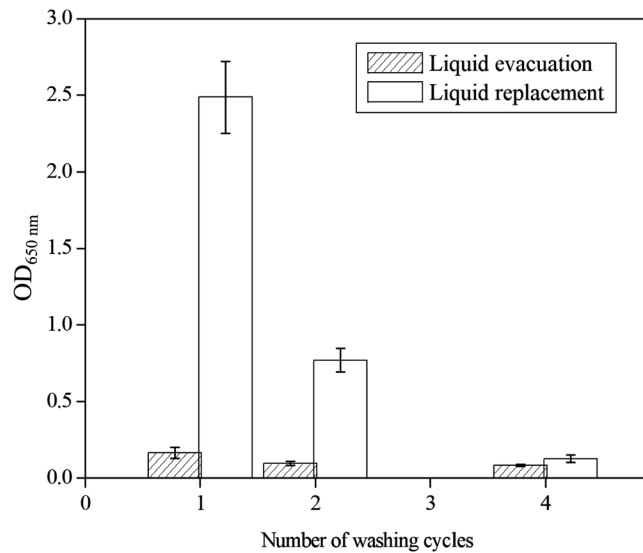


FIG. 5. The comparison of washing efficiency between liquid-replacement and liquid-evacuation approaches. The liquid-evacuation approach shows lower background signals compared to the liquid-replacement approach.

decreases as the product of $\bar{R}\Delta R d_H$ increases with a slope of -0.497 , which is very close to the theoretical prediction of the slope (-0.5). Therefore, the critical rotational speed can be estimated from the theoretical prediction.

To evaluate the washing efficiency of the liquid-evacuation approach, experiments were carried out by comparing the background signals of the assays between the liquid-evacuation and the liquid-replacement approaches. As shown in Fig. 5, for both approaches, the background signal decreases as the number of washing cycle increases. In addition, the liquid-evacuation approach shows superior washing efficiency to the liquid-replacement approach. The background signal of the assay washed one time using the liquid-evacuation approach is equivalent to the one washed four times using the liquid-replacement approach. One of the possible explanations is that in the liquid-replacement approach, the wash buffer mixed with the liquid residing in the reaction chamber during the draining process and a significant amount of the residue from the previously residing liquid still remained in the reaction chamber. As a result, the reaction chamber needs to be washed four times by the liquid-replacement approach in order to lower the background signal of the assay. On the other hand, in the liquid-evacuation approach, most of the liquid residing in the reaction chamber was removed from the reaction chamber in the evacuation process so that when the wash buffer was added, the remaining residue in the reaction chamber could be removed easily and a low background signal could be achieved with one wash cycle. In conclusion, a decent washing efficiency with fewer washing cycles and lower wash buffer volume can be accomplished by the liquid-evacuation approach.

Magnetic module design

The magnetic module plays an important role in controlling the movement of the magnetic beads in both incubation and washing processes. As shown in Fig. 6(a), the magnetic module includes a stationary magnet stage and a moving magnet stage. The stationary magnet stage is composed of permanent magnets located in both inner and outer radial positions. The moving magnet stage contains eight moving rails with one moving magnet inside each moving rail. A microfluidic disk with magnetic beads is placed between the stationary and the moving magnet stages. In the incubation process, the disk was rotated at low rotational speed (ω_L) and the moving magnet would travel alternatively between the inner and outer radial positions of the moving rail due to the attraction of the stationary magnets as shown in Fig. 6(b). Since the moving magnet was located near

the magnetic beads, the magnetic beads would follow the motion of the moving magnet and promoted the reaction between the magnetic beads and the liquid in the reaction chamber. On the other hand, in the siphoning-evacuation process, the disk was rotated at high rotational speed (ω_H) so that the moving magnet moved to the outer radial position of the moving rail and kept the magnetic beads inside the reaction chamber during the liquid draining process [Fig. 6(c)]. Hence, both the movement of the magnetic beads and liquid flow in the incubation and washing processes can be coordinated by controlling the rotational speed of the disk.

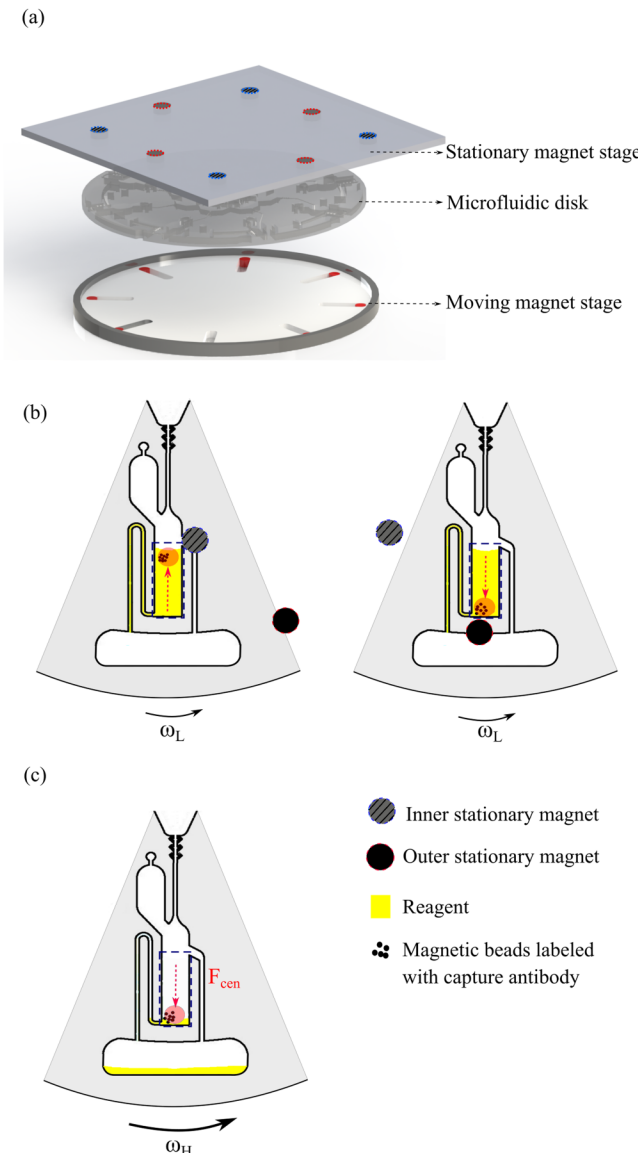


FIG. 6. The schematic illustration of the magnetic module which assisted the movement of the magnetic beads in both incubation and washing processes. (a) The magnetic module included the stationary magnet stage, the moving magnet stage, and the microfluidic disk. (b) In the incubation process, the disk was rotated at a low rotational speed and the moving magnet traveled alternatively between the inner and the outer radial positions of the moving rail by the attraction of the stationary magnets. (c) In the washing process, the disk was rotated at a high rotational speed and the moving magnet stayed at the outer radial position of the moving rail. The magnetic beads were kept inside the reaction chamber as the liquid flowed into the waste chamber.

TABLE I. Procedure of disk-based ELISA by the LASE technique.

Spin No.	Speed (RPM)	Time (s)	Operation
1	0	10	Loading samples and reagents (MB-Ab, Ab-HRP)
2	4000	10	Delivering samples and reagents into reaction chambers
3	10	3600	Incubation and priming the siphoning channel
4	4000	100	Evacuating the liquid in the reaction chamber
5	0	10	Loading wash buffer
6	4000	10	Aliquoting and delivering the wash buffer into reaction chambers
7	10	60	Priming the siphoning channel
8	4000	10	Evacuating the liquid in the reaction chamber
9	0	10	Loading TMB substrate
10	4000	10	Aliquoting and delivering the TMB substrate into the reaction chambers
11	10	900	Color development
12	10	60	Detection

Disk-based ELISA by the LASE technique

The procedure of the disk-based ELISA by the LASE technique is shown in Table I. The estimated assay time is 80 min approximately. The volumes used for the sample, the magnetic beads labeled with the capture antibody, and the detection antibody labeled with HRP in each test are 50 μl , 1 μl , and 1 μl , respectively. The volumes used for the wash buffer and TMB substrate are 400 μl in each assay.

The disk-based ELISA by the LASE techniques was used to perform human chorionic gonadotropin (hCG) detection, and the test results were compared with the assays conducted using microtiter plates. As shown in Fig. 7, the test results from both approaches show a similar trend. However, the disk-based ELISA with the LASE technique demonstrates the ability to simplify the sample loading steps, reduce the volume of reagents required in each assay, and shorten the assay time (80 min vs. 3 h). Moreover, the incubation and siphoning-evacuation washing processes can be performed automatically by a low-cost spinning system.

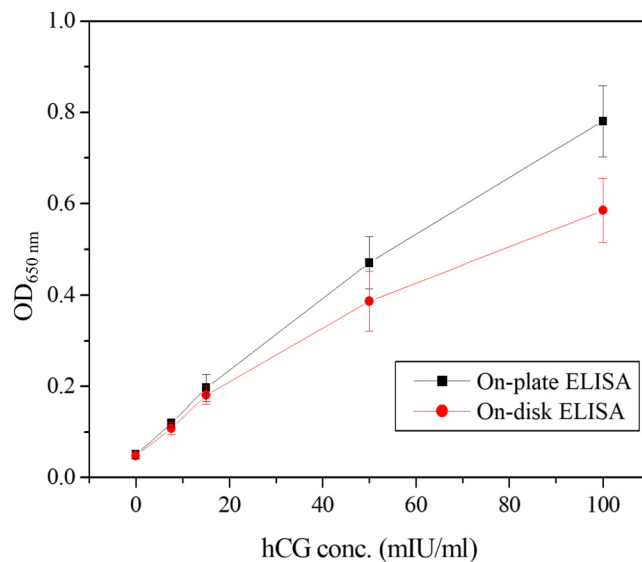


FIG. 7. The comparison of the test results between disk-based ELISA and the ELISA conducted using microtiter plates.

CONCLUSIONS

A disk-based ELISA with the LASE technique, which is able to facilitate the reagent loading procedure through aliquoting, promote incubating reaction through the magnetic module, and improve the efficiency of washing by the siphoning evacuation, was developed in this work. In addition, the entire ELISA protocol can be carried out using a two-step spinning protocol, which can be performed by a low-cost motor. In this study, the liquid flow control for incubation and evacuation by coordinating the disk rotation and the siphoning effect are demonstrated. The experimental results show that the washing efficiency of the assay by the liquid-evacuation approach is superior to the liquid-replacement approach. In addition, disked-based ELISA with the LASE technique would show better performance when a large number of assays were integrated on one disk by reducing the time and labor required for reagent loading and liquid handling processes. Although only 8 assay fluidics were demonstrated in the current disk design, the number of assay fluidics can be further increased by enlarging the diameter and the thickness of the disk. However, the number of the assay fluidics is still limited by the space required for the waste chambers since they have to accommodate the total volume of reagents and wash buffers used in each assay. It is believed that this system provides a more affordable and automatic way to carry out immunoassays.

ACKNOWLEDGMENTS

The authors thank the Ministry of Science and Technology of Taiwan (MOST) for the financial support (Grant No. 106-2221-E-035-078).

- ¹Y. Ukita, Y. Utsumi, and Y. Takamura, "Direct digital manufacturing of a mini-centrifuge-driven centrifugal microfluidic device and demonstration of a smartphone-based colorimetric enzyme-linked immunosorbent assay," *Anal. Methods* **8**(2), 256–262 (2016).
- ²Y. Ukita *et al.*, "Stacked centrifugal microfluidic device with three-dimensional microchannel networks and multifunctional capillary bundle structures for immunoassay," *Sens. Actuators B Chem.* **166–167**, 898–906 (2012).
- ³H. He *et al.*, "Design and testing of a microfluidic biochip for cytokine enzyme-linked immunosorbent assay," *Biomicrofluidics* **3**(2), 022401 (2009).
- ⁴S. Lai *et al.*, "Design of a compact disk-like microfluidic platform for enzyme-linked immunosorbent assay," *Anal. Chem.* **76**(7), 1832–1837 (2004).
- ⁵H. Kido, A. Maquieira, and B. D. Hammock, "Disc-based immunoassay microarrays," *Anal. Chim. Acta* **411**(1–2), 1–11 (2000).
- ⁶H.-C. Wu *et al.*, "Design and analysis of a robust sequential flow control using burst valves on the centrifugal platform," *J. Nanosci. Nanotechnol.* **16**(12), 12602–12608 (2016).
- ⁷C.-H. Shih *et al.*, "An enzyme-linked immunosorbent assay on a centrifugal platform using magnetic beads," *Biomicrofluidics* **8**(5), 052110 (2014).
- ⁸T. H. G. Thio *et al.*, "Sequential push-pull pumping mechanism for washing and evacuation of an immunoassay reaction chamber on a microfluidic CD platform," *PLoS ONE* **10**(4), e0121836 (2015).
- ⁹T.-H. Kim *et al.*, "Flow-enhanced electrochemical immunosensors on centrifugal microfluidic platforms," *Lab Chip* **13**(18), 3747–3754 (2013).
- ¹⁰A. Kazemzadeh *et al.*, "Gating valve on spinning microfluidic platforms: A flow switch/control concept," *Sens. Actuators B Chem.* **204**, 149–158 (2014).
- ¹¹B. S. Lee *et al.*, "Fully integrated lab-on-a-disc for simultaneous analysis of biochemistry and immunoassay from whole blood," *Lab Chip* **11**(1), 70–78 (2011).
- ¹²Z. Noroozi, H. Kido, R. Peytavi, R. Nakajima-Sasaki, A. Jasinskas, M. Micic, P. L. Felgner and M. J. Madou, *Rev. Sci. Instrum.* **82**(6), 064303 (2011).
- ¹³S. I. En Lin, "A novel splitter design for microfluidic biochips using centrifugal driving forces," *Microfluidics Nanofluidics* **9**(2–3), 523–532 (2010).
- ¹⁴B. S. Lee *et al.*, "A fully automated immunoassay from whole blood on a disc," *Lab Chip* **9**(11), 1548–1555 (2009).
- ¹⁵H. Nagai *et al.*, "A single-bead analysis on a disk-shaped microfluidic device using an antigen-immobilized bead," *Anal. Sci.* **23**(8), 975–979 (2007).
- ¹⁶N. Honda *et al.*, "Simultaneous multiple immunoassays in a compact disc-shaped microfluidic device based on centrifugal force," *Clin. Chem.* **51**(10), 1955–1961 (2005).
- ¹⁷W. S. Lee *et al.*, "Electrospun TiO₂ nanofiber integrated lab-on-a-disc for ultrasensitive protein detection from whole blood," *Lab Chip* **15**(2), 478–485 (2015).
- ¹⁸X. Meng *et al.*, "Conditional siphon priming for multi-step assays on centrifugal microfluidic platforms," *Sens. Actuators B Chem.* **242**, 710–717 (2017).
- ¹⁹M. Keller *et al.*, "Robust temperature change rate actuated valving and switching for highly integrated centrifugal microfluidics," *Lab Chip* **17**(5), 864–875 (2017).
- ²⁰D. J. Kinahan *et al.*, "Baking powder actuated centrifugo-pneumatic valving for automation of multi-step bioassays," *Micromachines* **7**(10), 175 (2016).

- ²¹S. Zehnle *et al.*, “Pneumatic siphon valving and switching in centrifugal microfluidics controlled by rotational frequency or rotational acceleration,” *Microfluidics Nanofluidics* **19**(6), 1259–1269 (2015).
- ²²F. Schwemmer *et al.*, “A microfluidic timer for timed valving and pumping in centrifugal microfluidics,” *Lab Chip* **15**(6), 1545–1553 (2015).
- ²³J. Siegrist *et al.*, “Serial siphon valving for centrifugal microfluidic platforms,” *Microfluidics Nanofluidics* **9**(1), 55–63 (2010).
- ²⁴C.-H. Lin *et al.*, “A point-of-care prothrombin time test on a microfluidic disk analyzer using alternate spinning,” *J. Nanosci. Nanotechnol.* **15**(2), 1401–1407 (2015).
- ²⁵T. Brenner *et al.*, “Frequency-dependent transversal flow control in centrifugal microfluidics,” *Lab Chip* **5**(2), 146–150 (2005).
- ²⁶S. J. Oh *et al.*, “Centrifugal loop-mediated isothermal amplification microdevice for rapid, multiplex and colorimetric foodborne pathogen detection,” *Biosens. Bioelectron.* **75**, 293–300 (2016).